Supporting information

Stabilizing Metastable Polymorphs of Metal-Organic Frameworks through Encapsulating Graphene Oxide and Mechanistic Studies

Hui Su,[a,b] Yao Du, [a] Jichuan Zhang, [a] Panpan Peng, [a] Shenghua Li,*[a] Pengwan Chen,[b] Michael Gozin,[c] and Siping Pang,*[a]

[a]School of Materials Science & Engineering, Beijing Institute of Technology, Beijing 100081, PR China

[b]State key laboratory of explosion science and technology, Beijing Institute of Technology, Beijing 100081, PR China

[c]School of Chemistry, Faculty of Exact Science, Tel Aviv University, Tel Aviv, 69978, Israel

Corresponding Author

*E-mail: lishenghua@bit.edu.cn

pangsp@bit.edu.cn

1 Instruments and methods for measurements

(1) **Instrumentation:** Powder X-ray diffraction (PXRD) patterns of the samples were analyzed with monochromatized Cu-Kα (λ = 1.54178 Å) incident radiation by Bruker D8 Advance X-ray diffractometer operating at 40 kV voltage and 50 mA current. PXRD patterns were recorded from 5° to 90° (2θ) at 298 K. Infrared (IR) spectrum was recorded on a Bruker Tensor 27 spectro-photometer with HTS-XT (KBr pellets). Raman spectra (RS) in the 3500~50 cm-1 range were measured in back scattering geometry with a LabRAM HR Evolution Raman spectrometer. The 532 nm line was used as excitation with the resolution was 2 cm^{-1}. X-ray photoelectron (XPS) spectrum was recorded on an AXIS Ultra X-ray photoelecton spectroscopy (Kratos corporation, England). Elemental analysis was performed on an Elementar Vario EL (Germany). Field emission scanning electron microscopy (FE-SEM, Hitachi S-4800) was used to characterize the morphology (5 KV accelerating voltage, gold coating) and element analysis (at 20 KV accelerating valtage) of the samples. Transmission electron microscopy (TEM; FEI Tecnai G2 F30) and atomic force microscopy (AFM; NanoScope V, VEECO) was used to observe the interphase structure of the hybrid.

(2) Measurement of heat of reaction and ignition temperature using DSC/TG: In our study, a TA-DSC Q2000 differential scanning calorimeter was employed to determine the ignition temperatures. About 1.5 mg of sample was used and the temperature was programmed to 500 ℃ (773 K) at the rate of 10 ℃ min-1 in 60 mL min^{-1} N_2 flow. The ignition temperature was usually regarded as the onset temperature of an exothermic reaction and also as the lowest temperature that can induce the thermal explosion of a sample.

(3) Measurement of impact sensitivity: The impact sensitivity was tested on a type 12 tooling according to "up and down" method (Bruceton method). A 2.5 kg weight was dropped from a set height onto a 20 mg sample placed on 150 grit garnet sandpaper. Each subsequent test was made at the next lower height if explosion occurred and at the next higher height if no explosion happened. 50 drops were made from different heights, and an explosion or non-explosion was recorded to determine the results. RDX was considered as a reference compound, the impact sensitivity of RDX is 7.4 J.

(4) Measurement of friction sensitivity: The friction sensitivity was tested on a FSKM-10 BAM friction apparatus. RDX was also used as a reference compound, and its friction sensitivity is 110 N.

(5) Measurement of electrostatic sensitivity: The electrostatic sensitivity was tested on a FSKM 50/20K apparatus produced by OZM Research. The sample was placed between the porcelain plate and peg. The weight of leading at least one ignition in six times was recorded. The friction sensitivity of RDX is 0.2 J. Test conditions: 25 ℃ (temperature); 34% (relative humidity).

(6) The measurement of the heat of detonation (ΔH_{det})

To estimate the heat of detonation (ΔHdet) of the above materials, and to see how they compare to those of common energetic materials, a precise rotating-oxygen bomb calorimeter31 was used for energetic MOF(ATA-a) and GO⊂MOF(ATA-a). The heats of reaction of gram-scale thermites (500 mg sample) were measured using a Parr 6200 (Parr Instrument Company, USA) bomb calorimeter under the oxygen atmosphere at 3 MPa. The measured heats of reaction of MOF(ATA-a), GO⊂MOF(ATA-a) and GO/MOF(ATA-a) are 8.8624 kJ g^{-1}, 8.8484 kJ g^{-1} and 8.9107 kJ g^{-1}, respectively. In addition, the chemical formula for GO⊂MOF(ATA-a)

approximately equal to MOF(ATA-a), which is due to the low GO content(<1 %) for GO⊂MOF(ATA-a).

On the basis of the formula $\Delta_cH_{\Theta m} = \Delta_cU_{\Theta m}$ + [ng (products) - ng (reactants)] RT (where ng is the total molar amount of gases in the products or reactants, R= 8.314 J mol^{-1} K^{-1}, T = 298.15 K), the standard molar enthalpies of combustion ($\Delta cH\Theta m$) can be derived as being 2082.4 kJ mol^{-1}. The combustion reaction Equations are listed as equations (1):

$$C_2H_5N_{10}Zn + 3.75\ O_2 = ZnO + 2\ CO_2 + 2.5\ H_2O + 5\ N_2 \quad (1)$$

The standard molar enthalpies of formation of the combustion products are obtained from the literature[1]. According to Hess's law, the standard molar enthalpies of formation ($\Delta^fH_{\Theta m}$) of MOF(ATA-a) at 298.15 K are calculatedas 340.4 kJ mol^{-1}, respectively. In accordance with the maximum heat release principle, zinc, methane, nitrogen and carbon ere assumed to be the final products of decomposition of the organic part of the framework MOF(ATA-a), and the formation of zinc was assumed to be governed by the deficiency of oxygen. The complete detonation reactions are described by equations (2):

$$C_2H_5N_{10}Zn = Zn + 1.25CH_4 + 5\ N_2 + 0.75\ C \quad (2)$$

In the theoretical case, the heat of detonation ($\Delta Hdet$) of compounds MOF(ATA-a), GO⊂MOF(ATA-a) and GO/MOF(ATA-a) at 298.15 K are calculated as 1858.2 J g^{-1}, 1906.5 J g^{-1} and 1891.5 J g^{-1}, respectively.

2 Figures and table

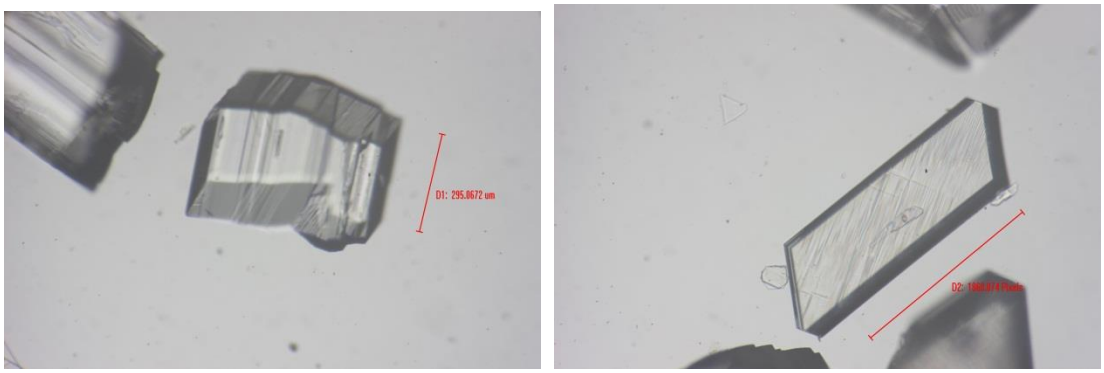

Figure S1. Photograph for preparated MOFs(ATA-a) and MOFs(ATA-b) ((MOF(ATA-a): left; MOF(ATA-b): left right)

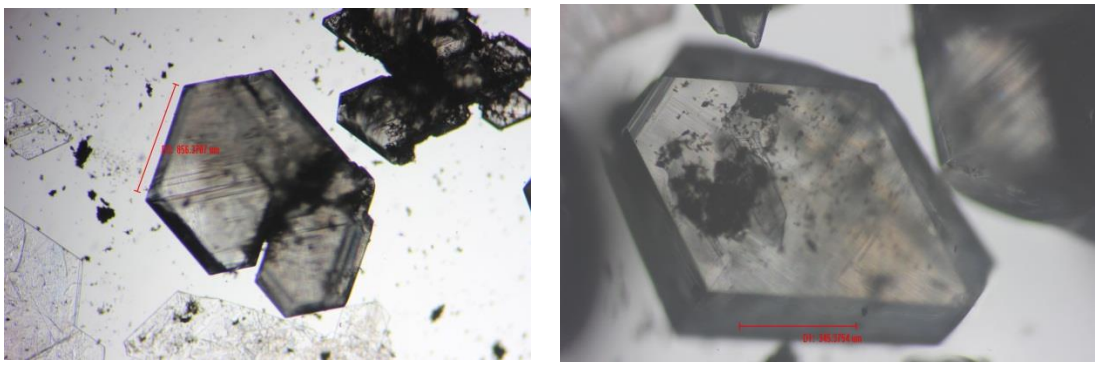

Figure S2. Photograph for new preparated GO⊂MOFs(ATA-a) and GO⊂MOFs(ATA-b) (GO⊂ (MOF(ATA-a): left; GO⊂MOF(ATA-b): left right)

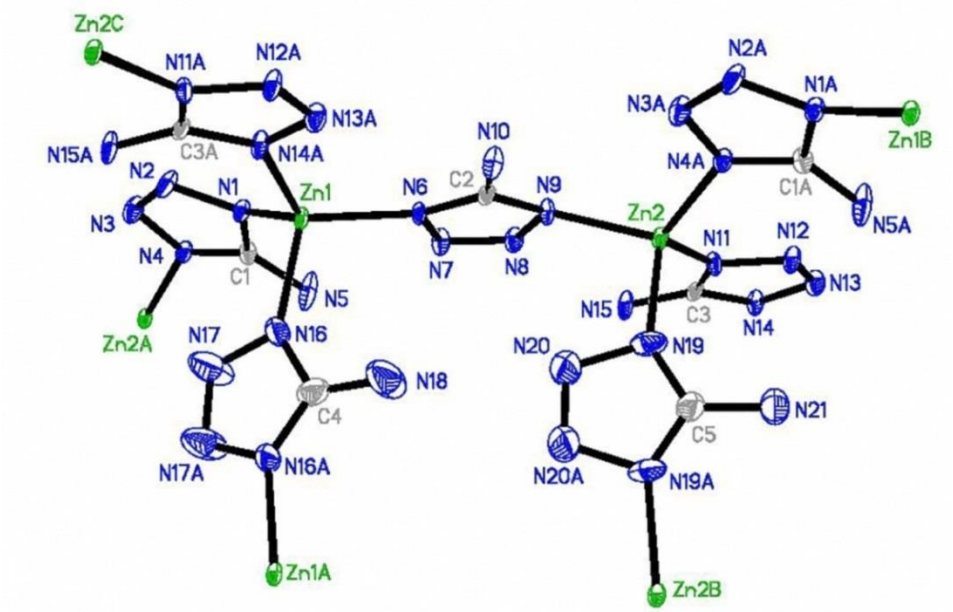

Figure S3. The ortep drawing shows the coordination for MOFs(ATA-a) (MOFs(ATA-a) and MOFs(ATA-b) with identical coordination mode)[2]. Displacement ellipsoids are drawn at the 40% probability level and H atoms are omitted for clarity.

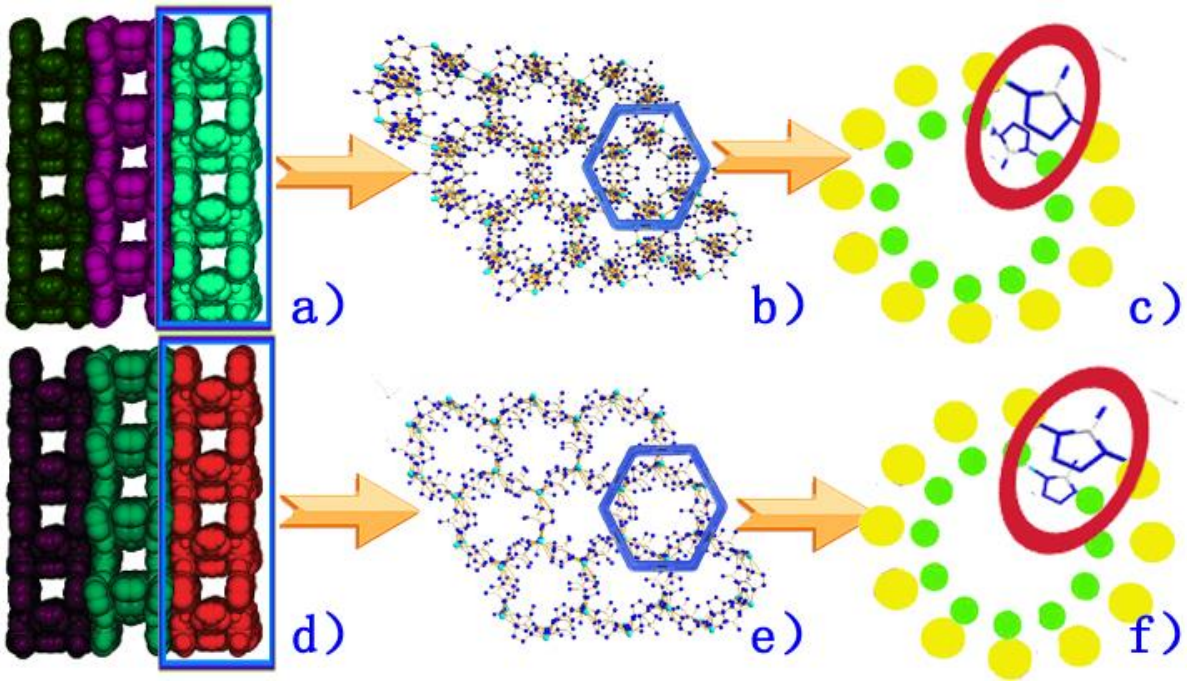

Figure S4. Schematic view about structural differences between MOF(ATA-a) and MOF(ATA-b). (MOF(ATA-a), upper panel; MOF(ATA-b), lower panel. The difference between MOF(ATA-a) and MOF(ATA-b) is the ligand of ATA, which is parallel for MOF(ATA-b) and anti-parallel for MOF(ATA-b). Some atoms and structures have been omitted or replaced.

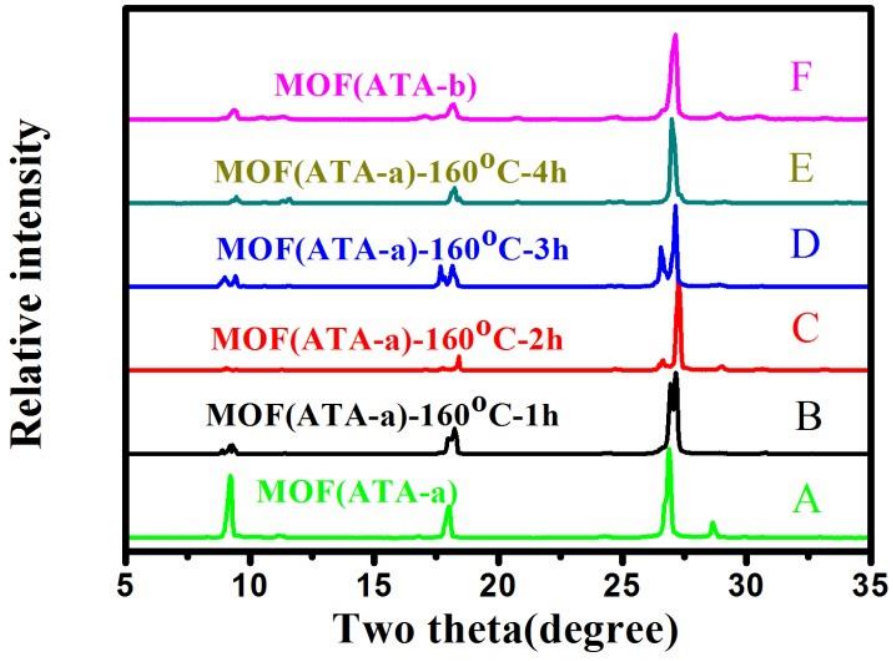

Figure S5. PXRD patterns of some materials: (a) pristine MOF(ATA-a), (b) MOF(ATA-a) placed 1hours at 160 ^{o}C, (c) MOF(ATA-a) placed 2 hours at 160 ^{o}C, (d) MOF(ATA-a) placed 3 hours at 160 ^{o}C, (e) MOF(ATA-a) placed 4 hours at 160 ^{o}C and (f) pristine MOF(ATA-b)

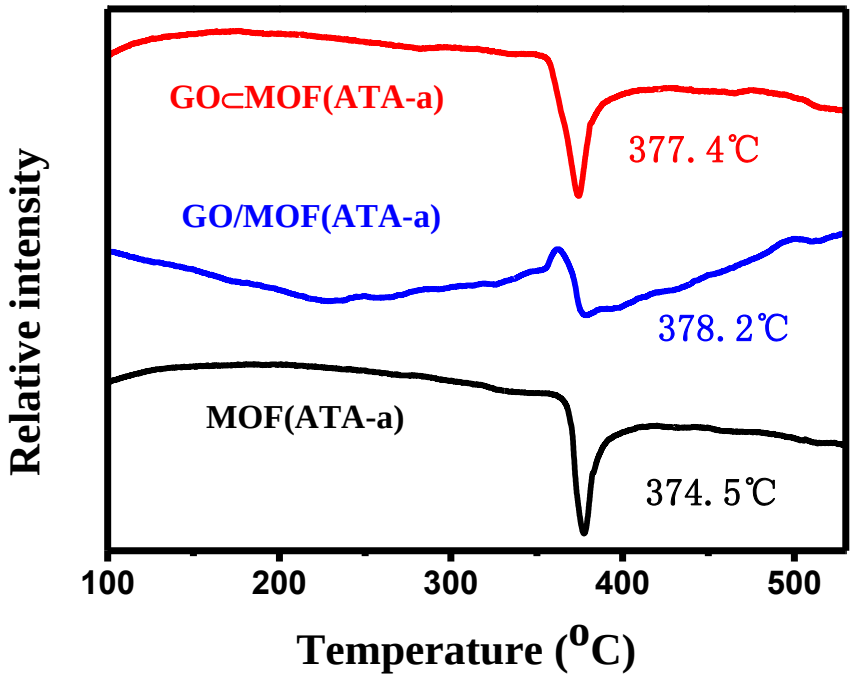

Figure S6. DSC curves of pristine MOF(ATA-a), GO/MOF(ATA-a) and GO⊂MOF(ATA-a).

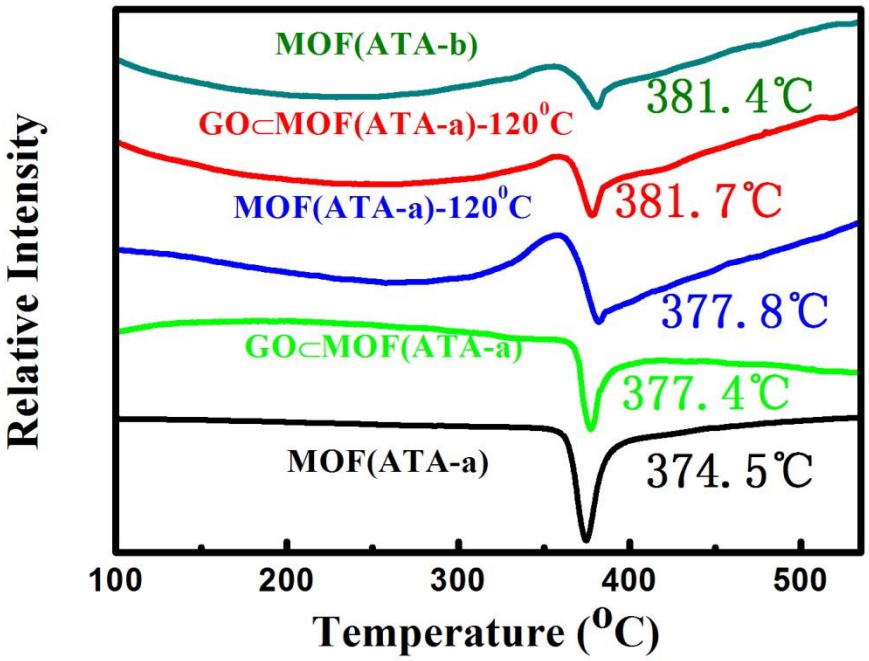

Figure S7. DSC curves of (A) pristine MOF(ATA-a), (B) GO/MOF(ATA-a), (C) MOF(ATA-a) at 120 °C for 10 h; (D) GO⊂MOF(ATA-a) at 120 °C for 48 h ; (E) pristine MOF(ATA-B)

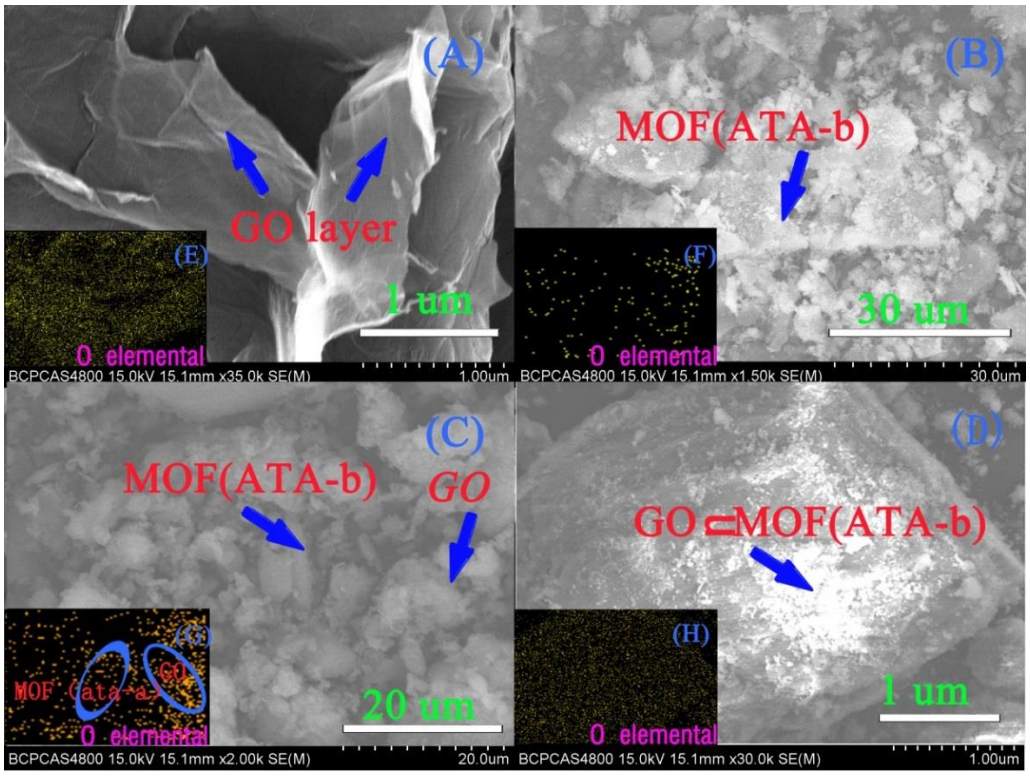

Figure S8. SEM images of (A) pristine GO, (B) pristine MOF(ATA-b), (C) GO/MOF(ATA-b) and (D)GO⊂MOF(ATA-b); EDS elemental maps of O for (E) pristine GO, (F) pristine MOF(ATA-b), (G) GO/MOF(ATA-b) and (H)GO⊂MOF(ATA-b)

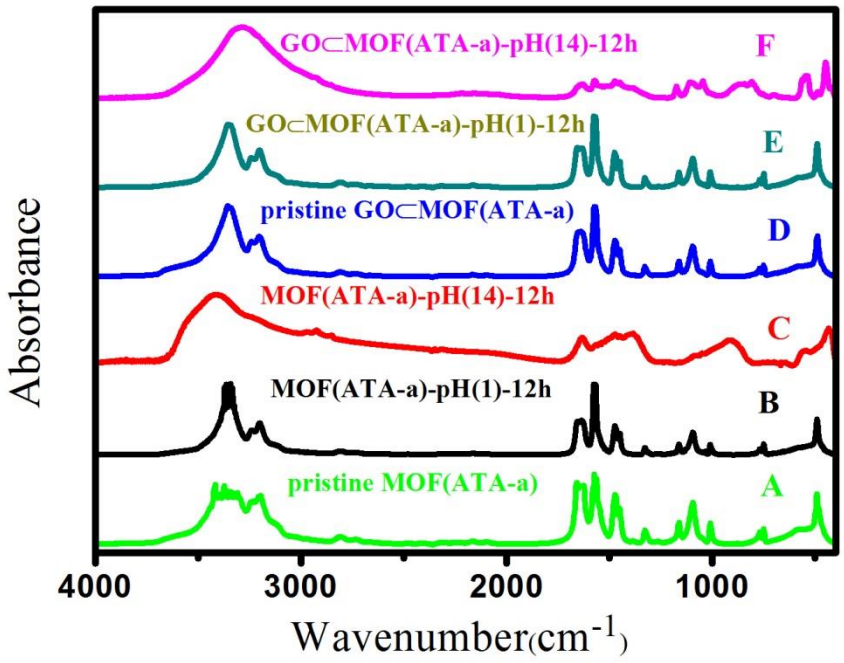

Figure S9. IR spectroscopy of MOF(ATA-a) and MOF(ATA-b) under different conditions. (A) pristine MOF(ATA-a); (B) MOF(ATA-a) in aqueous solutions with pH=1 for 10 h; (C) MOF(ATA-a) at 120 ^{o}C for 10 h; (D) MOF(ATA-a) at 160 ^{o}C for 5h, and (E) pristine MOF(ATA-a).

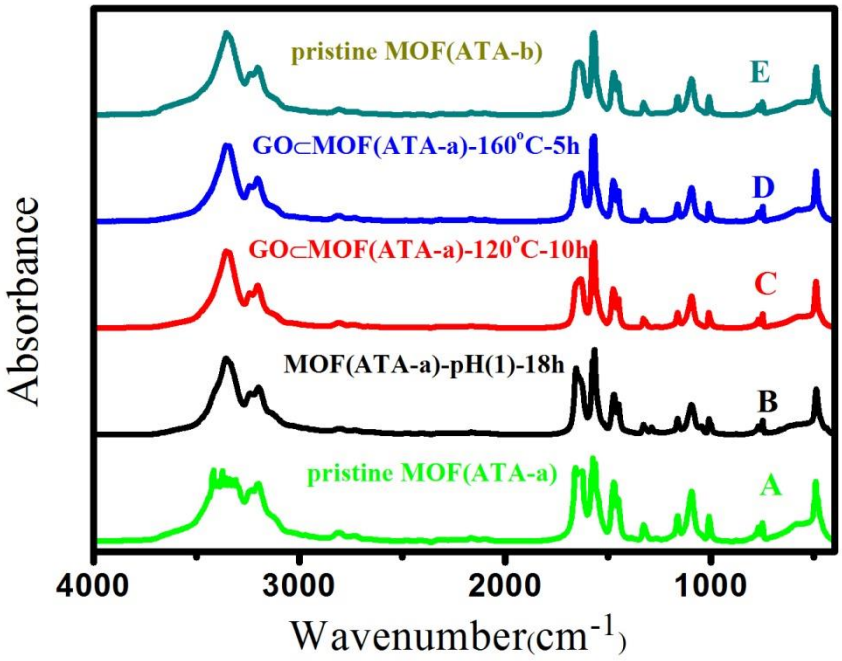

Figure S10. IR spectroscopy of MOF(ATA-a) and GO⊂MOF(ATA-a) under different conditions. (A) pristine MOF(ATA-a); (B) MOF(ATA-a) in aqueous solutions with pH=1 for 12 h; (C) MOF(ATA-a) in aqueous solutions with pH=14 for 12 h; (D) pristine GO⊂MOF(ATA-a); (E) GO⊂MOF(ATA-a) in aqueous solutions with pH=1 for 12 h, and (F) GO⊂MOF(ATA-a) in aqueous solutions with pH=14 for 12 h.

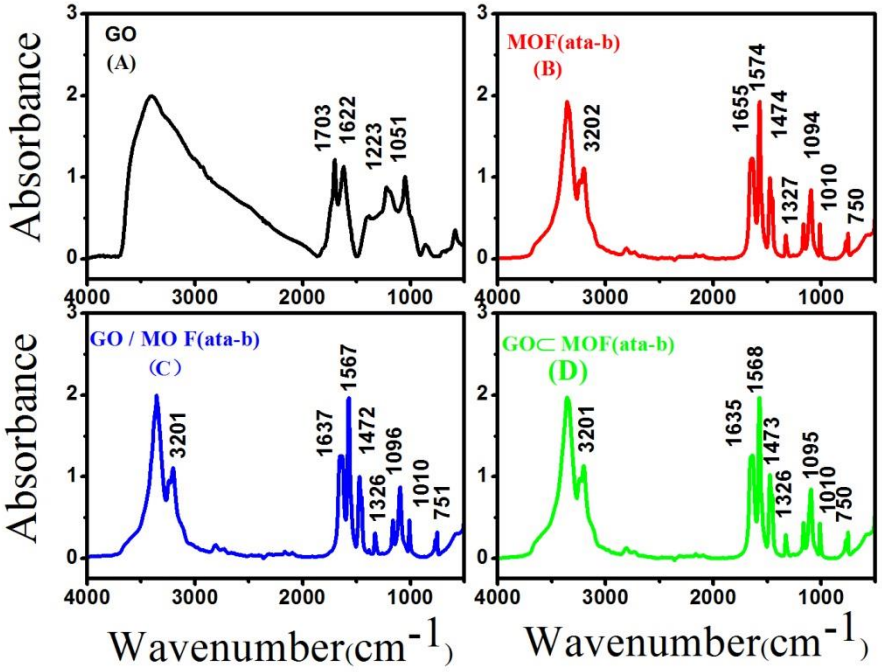

Figure S11. IR spectroscopy of (a) pristine GO, (b) pristine MOF(ATA-b), (c) GO/MOF(ATA-b) and (d) GO⊂MOF(ATA-b).

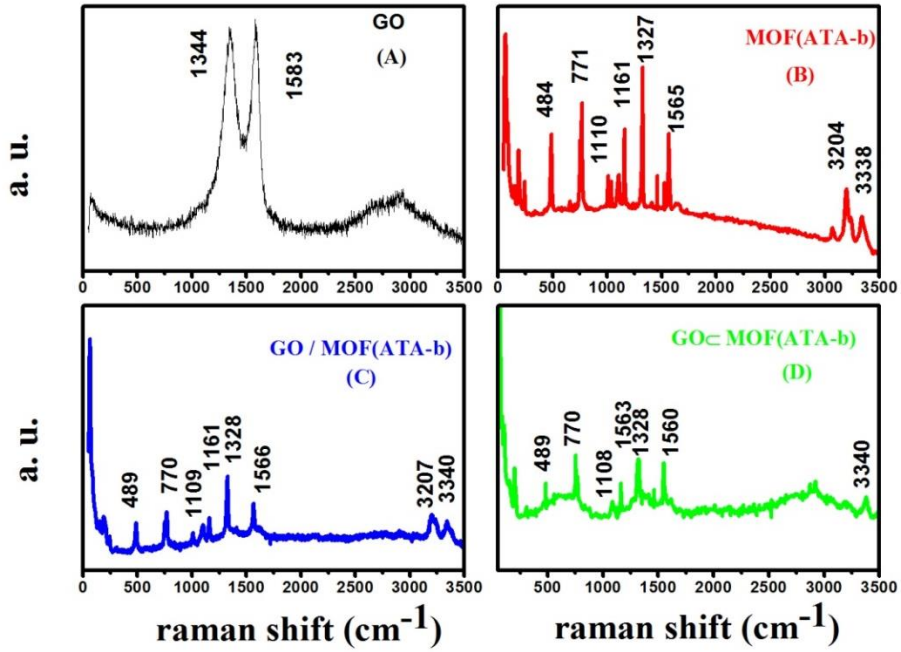

Figure S12. Raman spectroscopy of (a) pristine GO, (b) pristine MOF(ATA-b), (c) GO/MOF(ATA-b) and (d) GO⊂MOF(ATA-b)

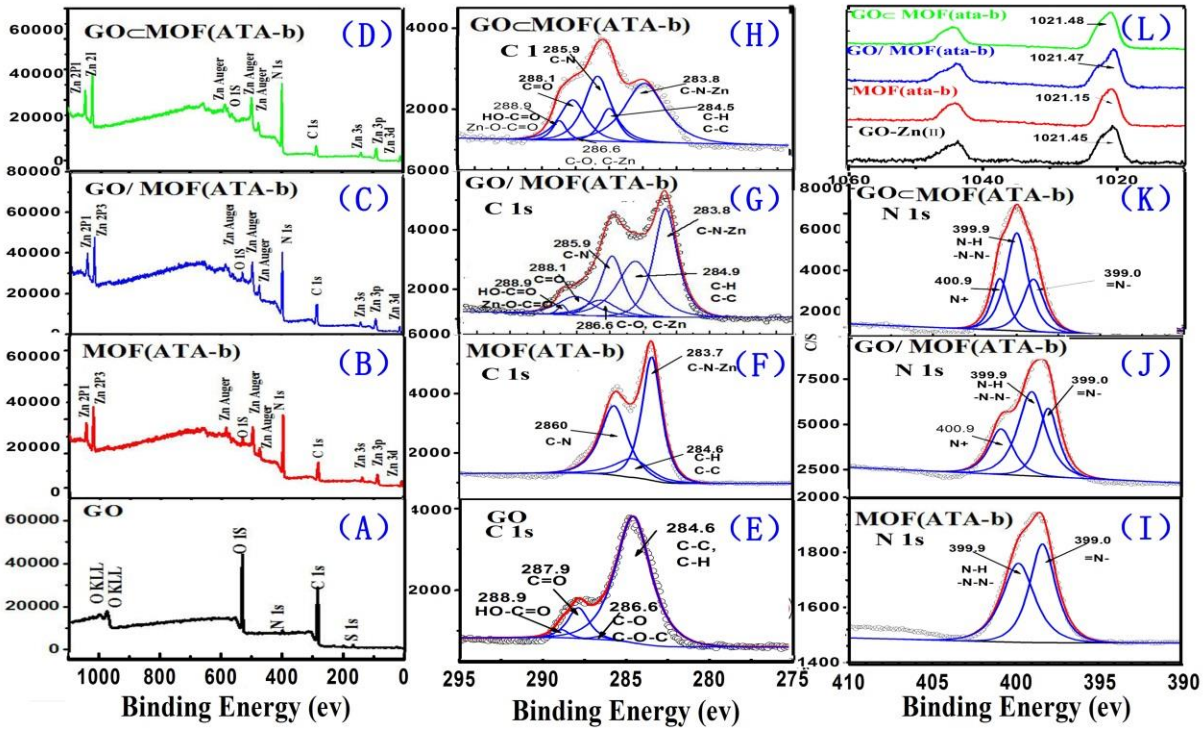

Figure S13. XPS binding energy spectra of (A) pristine GO, (B) pristine MOF(ATA-b), (C) GO/MOF(ATA-b) and (D)GO⊂MOF(ATA-b); the fitted C 1s peak curves for (E) pristine GO; (F) pristine MOF(ATA-b), (G) GO/MOF(ATA-b) and (H) GO⊂MOF(ATA-b); the fitted N 1s peaks for (I) pristine MOF(ATA-b), (J) GO/MOF(ATA-b) and (K) GO⊂MOF(ATA-b); and the Zn 2p spectrum for (L) GO-Zn(II), MOF(ATA-b), GO/MOF(ATA-b), and GO⊂MOF(ATA-b), without peak fitting.

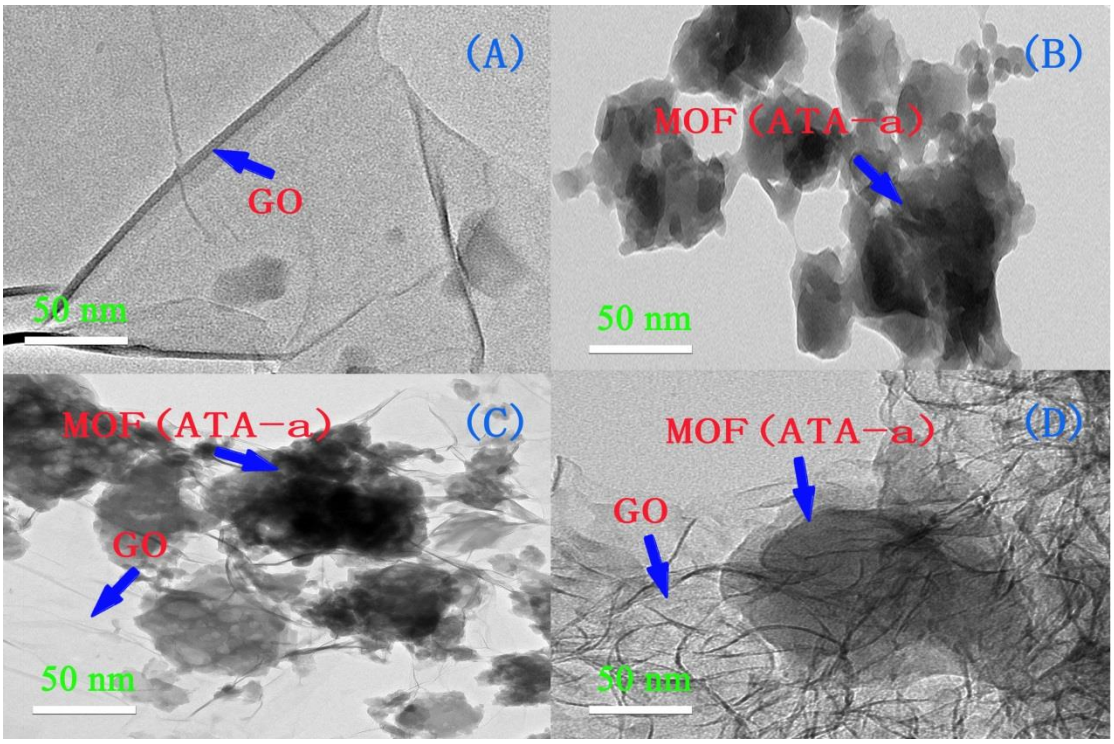

Figure S14. TEM images of (a) pristine GO, (b) pristine MOF(ATA-b), (c) GO/MOF(ATA-b) and (d)GO⊂MOF(ATA-b)

Table S1. Crystal data and structure refinement details for ATA-based complexes

Compound name	**MOF(ATA-a)**	**MOF(ATA-b)**
CCDC no.	1843046	-
Formula	$C_2H_5N_{10}Zn$	$C_2H_5N_{10}Zn$
T /K	293 (2)	173(2)
M	233.5	233.5
Crystal system	monoclinic	orthorhombic
Space group, Z	C 1 2/m 1 (12)	C m c m (63)
a /Å	10.3782(7)	17.8673(12)
b /Å	17.942(2)	10.4029(9)
c /Å	10.3758(8)	19.8430(16)
α /°	90	90
β /°	98.467(8)	90
γ /°	90.00	90
V / Å^3	1911.0(3)	3688.3(5)
μ(Mo-Kα) / mm^{-1}	2.546	2.638
D_{calc}/g cm^{-3}	1.623	1.682
2θmax /°	52	50.6
Measd/ Unique reflns	4495 / 1756	9183/1519
R_{int}	0.0347	0.0431
Parameters refined	212	259
R_1, wR_2 [I > 2σ(I)]	0.0368, 0.1087	0.0528, 0.1860
R_1, wR_2 (all data)	0.1114, 0.0410	0.0642, 0.1950
Max, min peak /e Å^{-3}	0.640, -0.562	0.652, -1.207

References

1. Speight, J. G., Lange's handbook of chemistry. McGraw-Hill New York: **2005**; *Vol. 1*.

2. Wang, X−W.; Chen, J-Z.; Liu, J-H. Photoluminescent Zn(II) Metal−Organic Frameworks Built from Tetrazole Ligand: 2D Four-Connected Regular Honeycomb (4363)-net. *Crystal Growth & Design*, **2007**, *7*,1227-1229.